Amino Acid Side Chain Descriptors for Quantitative Structure-Activity Relationship Studies of Peptide Analogues

Elizabeth R. Collantes and William J. Dunn III*

Department of Medicinal Chemistry & Pharmacognosy, The University of Illinois at Chicago, 833 South Wood Street, M/C 781, Chicago, Illinois 60612

Received July 21, 1994[⊗]

This report describes a new set of amino acid side chain descriptors, the isotropic surface area (ISA), and the electronic charge index (ECI) relevant to peptide quantitative structure-activity relationship (QSAR) studies. These features are derived from optimized three-dimensional structures of the natural and unnatural amino acids. Since the descriptors are derived considering side chain three-dimensional structure, 3D-QSARs result. Using the method of partial least squares, 3D-QSARs of peptide sets were developed. A comparison of the results to those obtained with the principal properties or z-scales shows that the ISA and ECI are comparable for parameterizing the structural variability of the peptide series and represent an interesting alternative.

Introduction

Quantitative structure-activity relationship (QSAR) studies express the biological activity of compounds as a function of structural variation. Despite difficulties in the QSAR analyses of peptides and proteins, there have been several successful reports that describe molecular structure in a quantitative way.[1-7] Recently, it has become obvious that in order to develop meaningful quantitative models of structure-activity relationships, the three-dimensional structures of the active compounds must be considered in their description. Hence, Charton and Charton[8] determined the dependence of protein conformation upon the side chain structure of the amino acid residues using Chou-Fasman parameters. In another approach to structure-activity studies, Kidera et al.[9] collected 188 properties of the 20 natural amino acids and applied factor analysis to these to obtain 10 orthogonal factors that are most important for determining the three-dimensional structure of proteins. The study of Kidera et al.[9] was the precursor to the development of the principal properties, or z-values, of Hellberg et al.[10] Their peptide QSAR methodology is based on a parametrization of each amino acid occurring in a peptide chain with three z-values, which are linear combinations of the original measured variables and are proposed to be related to hydrophilicity, bulk, and electronic properties. The principal properties have been successfully used to construct peptide QSARs using partial least squares (PLS) regression.[10-14]

Despite the extension of the z-scales to unnatural amino acids,[13,14] they are still limited in that they do not allow a straightforward interpretation of the resulting QSAR in terms of the physicochemical factors that are important for biological activity. Since the z-scales were derived from macroscopic properties, conformation is not explicitly considered in their derivation.

One way to address the problem is to generate theoretical features that can be calculated from the three-dimensional structure of a molecule. Using such descriptors, 3D-QSARs result. In this work, descriptors are derived from the side chain surface area and atomic charges of the amino acids.

One descriptor is the isotropic surface area (ISA), proposed and developed by Grigoras[15] as the portion of the solute molecule which is accessible to nonspecific interactions with the solvent, water. ISA for a compound is computed by first forming its supermolecule, which consists of the solute and water molecules associated with hydratable function groups. There is evidence that water forms hydrogen bonds in the gas phase with benzene.[16] We assume that the interactions between water and solute atoms, other than to those which act as classical hydrogen bond donors and acceptors, in an aqueous environment are nonspecific hydration. Hence, the solute surface which remains accessible to the nonspecific solvent interactions is the isotropic surface. ISA was found to be the main structural feature related to partition coefficients for a large number of organic solutes, providing a straightforward means to quantitate hydrophobicity from solute structure.[17]

In addition to ISA, the electronic charge index (ECI) of the side chain is proposed. ECI is the sum of the absolute value of the CNDO/2 charges of the side chain atoms. Buydens and Massart[18,19] showed that there is a correlation between the chromatographic retention of a series of solutes and the quantum chemical charge parameters related to the local polarity of the solutes.

ISA and ECI were derived, and QSAR methodologies were used to correlate structural variation with variation in activity for the sets of peptides analyzed previously by Hellberg et al.[10] The objective of this report is to explore the utility of ISA and ECI as parameters for 3D-QSAR studies of peptides.

Methods

Structures of Amino Acids. The structures of the 20 natural amino acids and their D-forms, including D-citrulline and D-penicillamine, were constructed with the BUILD and ISOMER options in the CHEMLAB-II v. 11.0 molecular modeling software.[20] The amino acids were modeled in their neutral forms. Conformational scans of the side chains were carried out as a function of the dihedral angle ψ. Geometries were optimized with the molecular mechanics option MMFF using the AMBER parameter set which is particularly suitable for amino acids and peptides.[21]

[⊗] Abstract published in *Advance ACS Abstracts*, June 1, 1995.

0022-2623/95/1838-2705$09.00/0

Table 1. Proposed Descriptors for the Natural Amino Acids

amino acid	ISA	ECI	amino acid	ISA	ECI
Gly	19.93	0.02	Asn	17.87	1.31
Ala	62.90	0.05	Glu	30.19	1.31
Val	120.91	0.07	Gln	19.53	1.36
Leu	154.35	0.10	Ser	19.75	0.56
Ile	149.77	0.09	Thr	59.44	0.65
Phe	189.42	0.14	Cys	78.51	0.15
Tyr	132.16	0.72	Met	132.22	0.34
Trp	179.16	1.08	Lys	102.78	0.53
Pro	122.35	0.16	Arg	52.98	1.69
Asp	18.46	1.25	His	87.38	0.56

Electronic Charge Index (ECI). After the structures were optimized, partial atomic charges were obtained with the CNDO/2 approximation.[22] The ECI used in this study is calculated as the sum of the absolute values of the charges q for each atom i present in the side chain of the amino acids:

$$\mathrm{ECI} = \sum |q_i|$$

ECI is a measure of the local polarity in the side chain R. A significant ECI contribution to activity may indicate the presence of a dipolar interaction of the side chain with the receptor.

Isotropic Surface Area (ISA). The program HYDRAT, developed in this laboratory, was used to build the supermolecule. It hydrates specific functional groups which are capable of H-bonding to form the hydrated supermolecule using empirical hydration rules.[15,23] Once the supermolecule is constructed, ISA is then calculated by summing the surfaces of the side chain atoms accessible to nonspecific solvent interactions. Surfaces which form the interface between waters of hydration and the solute are excluded from the ISA. ISAs were calculated with the modified version of the surface area program of Pearlman.[24]

PLS-QSAR. The method of partial least squares has been shown to be suitable in QSAR studies which seek to rationalize the structural features affecting the biological activity.[25,26] PLS regression seeks a relationship between a response or dependent variable, which is the vector **Y**, and descriptor data **X**. Latent variables are extracted both to model **X** and **Y** and to be optimally correlated. The PLS model consists of outer relations (**X** and **Y** block individually) and an inner relation linking both blocks:

$$Y_{i,j} = Y_j + \sum_{a=1}^{A} t_{i,a} p_{a,j} = e_{i,j}$$

$$X_{i,k} = X_k + \sum_{a=1}^{A} u_{a,i} q_{a,k} + e_{i,k}$$

The ts and us are correlated through the inner relation given below which leads to the estimation of the ys from the xs.

$$\hat{u} = bt$$

Different peptide analogues containing natural and unnatural amino acids were obtained from the paper of Hellberg et al.[10] Each varied amino acid position in the set was parameterized by ISA and ECI according to the amino acid sequence. Hence, the data matrices **X** for n dipeptides would have n rows for the training set and four columns, two descriptors for each amino acid. In all examples in this study, there is only one Y-variable.

Prior to the PLS analysis, the x-variables were mean-centered and scaled to unit variance. All PLS calculations were run using the UNIPALS software on a PC.[27]

Results and Discussion

Electronic Charge Index (ECI). Table 1 provides a list of the ECI for the side chains of the 20 common amino acids. It is a measure of the side chain polarity and not of the whole amino acid molecule. The largest

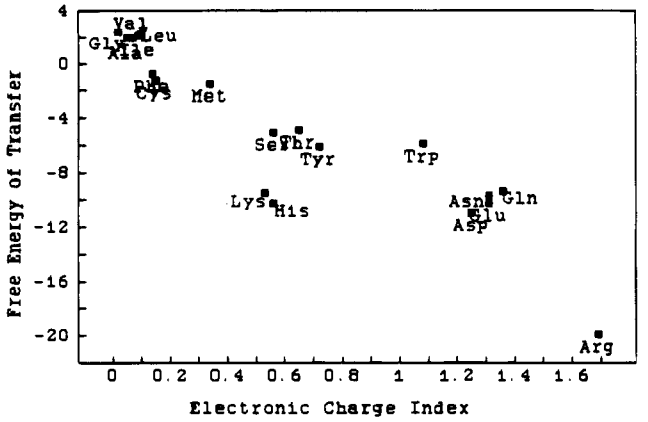

Figure 1. Relationship between ECI and ΔG_{vap}.

Table 2. Hydration for Amino Acid Structures

amino acid	no. of waters	amino acid	no. of waters
Gly	5	His	7
Ala	5	Lys	7
Val	5	Ser	7
Leu	5	Thr	7
Ile	5	Tyr	7
Phe	5	Asp	8
Cys	5	Glu	8
Met	5	Asn	10
Pro	5	Gln	10
Trp	6	Arg	11

ECI value is obtained for Arg which can be attributed to the guanido nitrogens in the side chain. The amide and carboxyl functionalities in side chains account for substantial charges on the respective amino acids.

ECI correlates well with the free energies of transfer of the free amino acids from the vapor phase to neutral aqueous solution (ΔG_{vap}) as shown in Figure 1 (r^2 = 0.81). The ΔG_{vap} values were taken from Wolfenden et al.[28] and reported at pH 7 assuming that only the uncharged compounds enter the gas phase. Correction was made for the fraction of the side chain that is ionized. Solutes in the vapor phase are assumed to be devoid of intermolecular contacts. Hence, the relationship indicates that the ECI characterizes the dipolar interactions of the amino acid side chains with the solvent water.

Isotropic Surface Area (ISA). Generation of the supermolecule relies on empirical rules of hydration for functional groups.[23] Hydration geometries allow three water molecules for the α-carboxyl group, while two waters are assigned to the α-amino group of each amino acid, for a total of five waters for the nonpolar amino acids. The other amino acids would have one or more waters associated with the side chain, depending on the functionality that is present. Table 2 gives the number of water molecules in the amino acid supermolecules.

The isotropic surface areas calculated from the supermolecule structures of the 20 natural amino acids are listed in Table 1. Inspection of the data shows that it is a measure of size. Glu has an ISA greater than Asp due to the additional methylene group. For side chains with functional groups capable of specific hydration, the proximity of water molecules further decreases the solvent accessibility with the result the ISAs are decreased. As an example, Ser which can be considered as the hydroxylated version of Ala, has a smaller ISA than Ala.

Comparison with Other Hydrophobicity Scales. ISA can be compared to the first principal property, z_1,

Table 3. Descriptor Scales z_1, z_2, and z_3 for the Natural Amino Acids

amino acid		z_1	z_2	z_3
Ala	A	0.07	−1.73	0.09
Val	V	−2.69	−2.53	−1.29
Leu	L	−4.19	−1.03	−0.98
Ile	I	−4.44	−1.68	−1.03
Pro	P	−1.22	0.88	2.23
Phe	F	−4.92	1.30	0.45
Trp	W	−4.75	3.65	0.85
Met	M	−2.49	−0.27	−0.41
Lys	K	2.84	1.41	−3.14
Arg	R	2.88	2.52	−3.44
His	H	2.41	1.74	1.11
Gly	G	2.23	−5.36	0.30
Ser	S	1.96	−1.63	0.57
Thr	T	0.92	−2.09	−1.40
Cys	C	0.71	−0.97	4.13
Tyr	Y	−1.39	2.32	0.01
Asn	N	3.22	1.45	0.84
Gln	Q	2.18	0.53	−1.14
Asp	D	3.64	1.13	2.36
Glu	E	3.08	0.39	−0.07

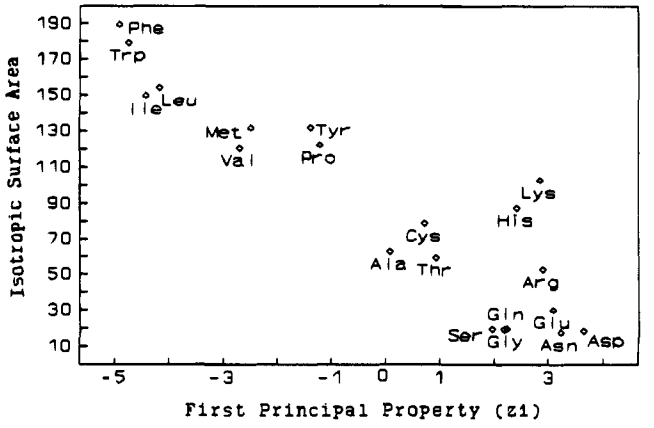

Figure 2. Plot of isotropic surface area and z_1.

proposed to be related to amino acid hydrophilicity. An inspection of the z-values given in Table 3 shows that Phe and Trp have the most negative z_1-values (−4.92 and −4.75, respectively) which indicate that, according to the z-scales, Phe is the least hydrophilic or most hydrophobic of the amino acids followed by Trp. On the other hand, Asp is the most hydrophilic since it has the most positive z_1-value (z_1 = 3.64). This is followed closely by Asn with z_1 of 3.22. Consistent with this z-scale, when the isotropic surface areas are arranged in increasing order, the largest ISA corresponds to Phe and the next largest is Trp. At the hydrophilic extremes are Asp and Asn whose ISAs are close to each other. The ISA values correlate with z_1 (Figure 2) with r^2 = 0.82.

As determined by Dunn et al.,[17] ISA accounted for 80% of the variation in partitioning data for 70 solutes in six partitioning systems. Hence, ISA is also compared to the amino acid hydrophobicity index reported by Fauchere and Pliska[28] and based on 1-octanol water partitioning of *N*-acetylamino acid amides. Figure 3 displays the relationship between ISA and π. In their π scale, Trp and Phe are the most hydrophobic (π_R = 2.25 and 1.79, respectively), a trend which parallels that obtained with ISA and z_1. The difference is that Trp is the more hydrophobic in the π scale. Radzicka and Wolfenden[30] determined that Phe remains the more hydrophobic, unless wet 1-octanol is used as the nonpolar reference phase in which case Trp appears to be the more hydrophobic.

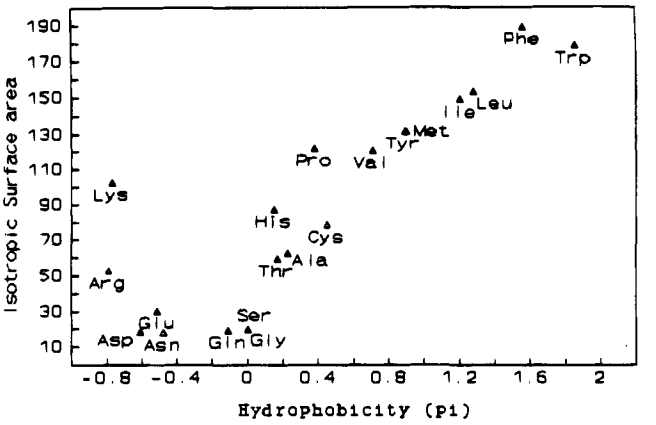

Figure 3. Plot of isotropic surface area and π values of Fauchere and Pliska.[23]

Table 4. Isotropic Surface Areas of the Tripeptides X-Phe-X

X	1	Phe	3	X	1	Phe	3
Gly	13.72	167.66	13.03	Asn	4.08	167.7	0
Ala	40.61	151.62	49.94	Glu	29.5	164.88	14.36
Val	126.48	138.05	109.57	Gln	20.63	127.41	9.55
Leu	136.74	140.92	143.01	Ser	22.68	149.85	30.63
Ile	153.72	130.09	131.67	Thr	62.46	115.94	52.53
Phe	164.58	114.93	168.84	Cys	94.06	152.75	94.16
Tyr	105.91	150.45	69.4	Met	156.47	140.78	146.54
Trp	164.13	113.17	88.83	Lys	81.36	139.97	94.71
Pro	96.29	158.24	67.11	Arg	35.94	125.28	45.87
Asp	19.1	158.99	15.61	His	47.84	128.87	51.79

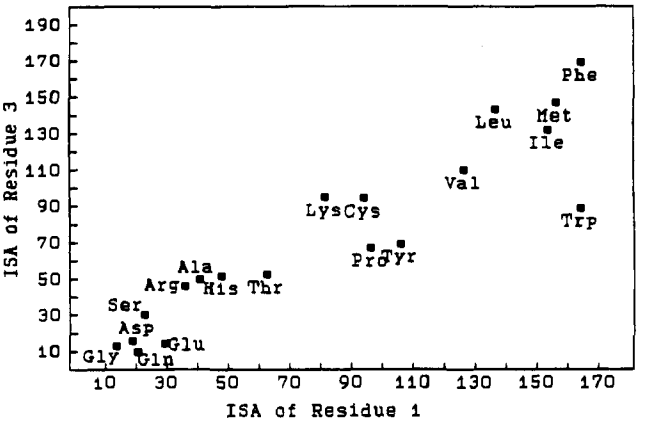

Figure 4. Plot of ISA of residue **1** vs residue **3** in tripeptide.

Positional Variation. Because the direct parametrization of peptides is quite difficult, most peptide QSAR models are developed using parameters derived from the amino acid. In order to explore the relationship between ISA and peptide conformation, a set of 20 tripeptides, X-Phe-X, was constructed in which X is a natural amino acid.

The tripeptides were generated from the optimized amino acid structures and further refined by conformational scan of the torsion angles on the Cα-atom. Phe was chosen as representative of an amino acid with a bulky, nonpolar side chain. After structure optimization, the peptides were hydrated and the resulting ISAs for the side chains were obtained.

As seen in Table 4, the ISAs of the side chains on either side of Phe vary, depending on whether the residue is in position 1 or 3. There is, however, good correlation between ISAs of the residues in positions 1 and 3 (r^2 = 0.87) as seen in Figure 4. Moreover, there is good correlation between the ISAs of the individual amino acids compared to the same amino acid when in the tripeptide. The data are plotted in Figure 5.

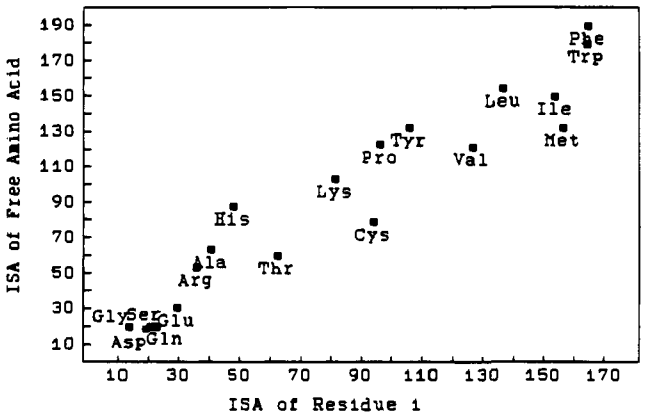

Figure 5. Plot of ISA of amino acid vs residue 1 in tripeptide.

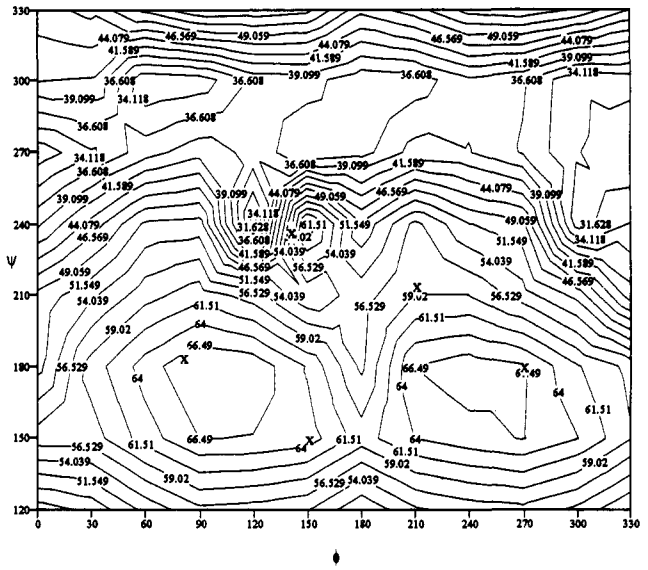

Figure 6. Iso-ISA contour plot of Ala residue in position 1 as a function of ϕ and ψ (represents minima).

The effect of variations in the main chain conformation on side chain ISA was further studied. In the tripeptide Ala-Phe-Ala, the torsional angles ϕ and ψ of the Ala residue were scanned separately in 30° increments while retaining fixed bond distances and angles in the rest of the molecule. The ISAs for conformations generated were then plotted as a function of $\phi-\psi$ as given in Figures 6 and 7, for Ala in positions 1 and 3, respectively. The locations of minimum-energy conformations are also marked in the figures. The contour maps show a variability in conformational distribution where regions of higher ISA values were observed to correspond to the low-energy regions at the locations of the Ala minima.

For the limited case of this tripeptide, the results show that even though ISA changes with conformation, the variability is internally consistent. To a first approximation for small peptides, as long as the descriptor is computed in an internally consistent manner, we propose that ISA can be used as variables for QSAR studies. This may explain why the z-values work even though they are derived from macroscopic properties in which conformational dependence is expressed as a Boltzmann average of many possible conformations. It also shows that variables computed on the amino acid structure can be transferred to peptides.

Using ISA and ECI, QSAR analyses of various peptide analogues were performed and compared with published results using the z-scales. Each varied amino acid

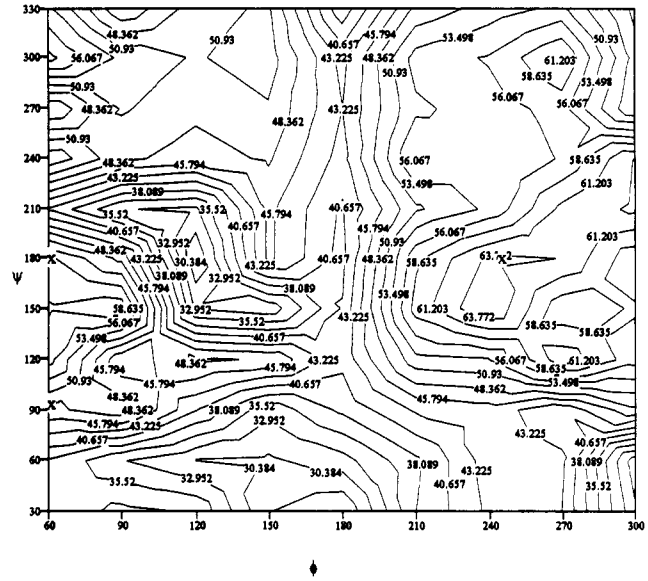

Figure 7. Iso-ISA contour plot of Ala residue in position 3 as a function of ϕ and ψ (represents minima).

position is described by ISA and ECI as listed in Table 1. The results obtained using the z-scales as reported are also presented and compared to the resulting PLS models developed with the proposed descriptors.

Peptides with Natural Amino Acids. Bradykinin-Potentiating Pentapeptides. A set of 15 bradykinin-potentiating pentapeptides, previously analyzed using the z-scales,[10] was obtained. The structural variation in this series was then described by ISA and ECI in each of the five amino acid positions. Thus, a descriptor matrix with 10 columns (five positions times two descriptors) and 15 rows (15 peptides) was obtained. Biological activity was reported as the logarithm of the relative activity index compared to the reference molecule (Val-Glu-Ser-Ser-Lys) whose activity was taken as 1.0. The PLS analysis gave a two-component model that explained 92% of the variance in the potentiating activity. The calculated activities for this training set of 15 bradykinin-potentiating peptides are given in Table 5. As can be seen, the differences between the predicted and measured activities are small with an overall residual standard deviation of 0.25.

The absolute magnitude of the PLS loadings reflects the relative importance of each variable. Thus, variables with high negative or positive PLS loadings are the most important ones in the model. From the plot of the **X**-variable loadings given in Figure 8, the highest contributions to the model are the ISA and ECI (indicated by 3 and 9, respectively) of the side chain substituted in site 3. These results are in agreement with earlier findings[31,32] that the presence of an aromatic amino acid residue in position 3 is essential for high activity. Since the loadings for both variables are positive, the substituent preferred at this position should be an amino acid which is large and highly polar. As seen in Table 1, Trp has both high ISA and ECI values, suggesting that the presence of Trp at position 3 will give a pentapeptide with good activity. From the data in Table 5, the pentapeptides with highest observed activity are indeed those with Trp in position 3, such as compound **6**.

Hellberg and co-workers[10] used the z-values to develop a QSAR for these data. Their analysis gave three significant PLS components which described 97% of the

Table 5. Biological Activity for Bradykinin-Potentiating Pentapeptides with **1**–**15** as Training Set and **16**–**31** as Test Set

		activity expressed as log RAI					
			$z_1z_2z_3$			ISA–ECI	
	peptide	obsd	calcd	pred	resd	calcd	pred	resd
1	VESSK	0.00	0.22			0.18		
2	VESAK	0.28	0.26			0.20		
3	VEASK	0.20	0.21			0.00		
4	VEAAK	0.51	0.25			0.02		
5	VKAAK	0.11	0.16			0.03		
6	VEWAK	2.73	2.57			2.55		
7	VEAAP	0.18	0.19			0.03		
8	VEHAK	1.53	1.58			1.51		
9	VAAAK	−0.10	−0.03			−0.02		
10	GEAAK	−0.52	−0.34			−0.56		
11	LEAAK	0.40	0.37			0.22		
12	FEAAK	0.30	0.35			0.45		
13	VEGGK	−1.00	−1.23			−0.58		
14	VEFAK	1.57	1.64			1.65		
15	VELAK	0.59	0.58			1.09		
16	AAAAA	−0.10		−0.43	0.33		−0.38	0.28
17	AAYAA	0.46		1.17	−0.71		1.49	−1.03
18	AAWAA	0.75		1.89	−1.14		1.06	−0.31
19	VAWAA	1.43		2.24	−0.81		2.51	−1.08
20	VAWAK	1.45		2.29	−0.84		2.51	−1.06
21	VKWAA	1.71		2.44	−0.73		2.56	−0.85
22	VWAAK	0.04		−0.16	0.20		0.12	−0.08
23	VAAWK	0.23		0.04	0.19		0.85	−0.62
24	EKWAP	1.30		1.82	−0.52		2.18	−0.88
25	VKWAP	2.35		2.42	−0.07		2.56	−0.21
26	RKWAP	1.98		2.11	−0.13		2.15	−0.17
27	VEWVK	1.71		2.64	−0.93		2.78	−1.07
28	PGFSP	0.90		0.91	−0.01		1.49	−0.59
29	FSPFR	0.64		1.57	−0.93		1.76	−1.12
30	RYLPT	0.40		0.00	0.40		0.98	−0.58
31	GGGGG	0.00		−2.11	2.11		−1.23	1.23

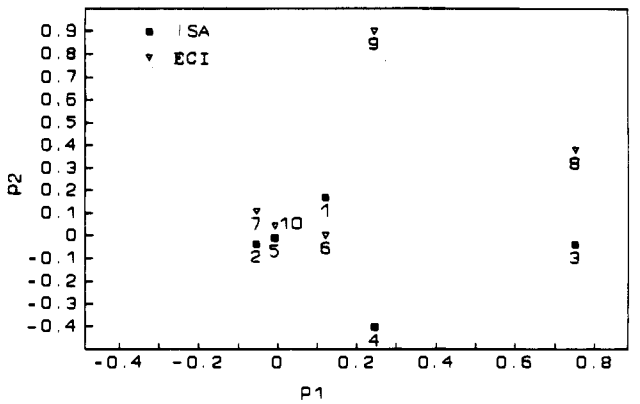

Figure 8. Plot of PLS loadings for bradykinin-potentiating pentapeptides.

variance in biological activity. The loadings indicate that position number 3 has the main influence on the activity. The predictive capability of the model developed on this training set of 15 bradykinin-potentiating pentapeptides was investigated using a test set of 15 active bradykinin-potentiating pentapeptides and an inactive one.[32] The results are listed in Table 5. Also included are the residuals which give a measure of the similarity between the new object and the training set. A residual standard deviation (RSD) of 0.84 was calculated for the z-scales compared to RSD of 0.82 for the new descriptors. A plot of the observed vs calculated/predicted bradykinin-potentiating activity for the ISA and ECI descriptors given in Figure 9 indicates good agreement between the observed and predicted activities for most of the analogues. Also plotted in Figure 9 are the predicted activities described by the z-values.

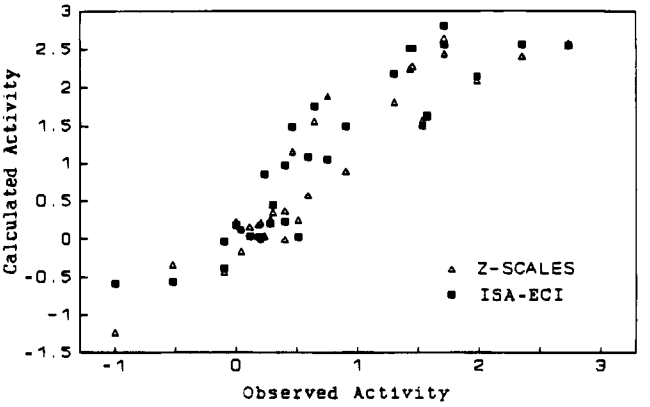

Figure 9. Plot of bradykinin-potentiating activities described by ISA–ECI and z-scales.

Table 6. Biological Activity of Bitter Tasting Dipeptides

			calcd log 1/T					calcd log 1/T	
no.	peptide	obsd log 1/T	$z_1z_2z_3$	ISA–ECI	no.	peptide	obsd log 1/T	$z_1z_2z_3$	ISA–ECI
1	GV	1.13	1.02	1.22	**25**	II	2.26	2.36	2.46
2	GL	1.68	1.35	1.54	**26**	IP	2.4	2.25	2.21
3	GI	1.7	1.32	1.49	**27**	IW	3.05	2.91	2.83
4	GP	1.35	1.21	1.25	**28**	IN	1.49	1.69	1.37
5	GF	1.8	1.68	1.86	**29**	ID	1.37	1.64	1.37
6	GW	1.89	1.87	1.87	**30**	IQ	1.49	1.69	1.39
7	GY	1.77	1.3	1.39	**31**	IE	1.37	1.59	1.48
8	AV	1.16	1.57	1.54	**32**	IK	1.65	1.64	2.07
9	AL	1.7	1.9	1.86	**33**	IS	1.49	1.58	1.31
10	AF	1.72	2.23	2.18	**34**	IT	1.49	1.62	1.68
11	VG	1.19	0.95	1.04	**35**	PA	1.32	1.7	1.47
12	VA	1.16	1.54	1.44	**36**	PL	2.22	2.28	2.31
13	VV	1.71	1.79	1.97	**37**	PI	2.33	2.26	2.27
14	VL	2	2.12	2.28	**38**	PY	1.8	2.23	2.17
15	LG	1.72	1.25	1.29	**39**	PF	2.8	2.61	2.64
16	LA	1.72	1.84	1.69	**40**	FG	1.77	1.54	1.55
17	LL	2.35	2.42	2.54	**41**	FL	2.87	2.71	2.8
18	LF	2.75	2.75	2.86	**42**	FP	2.7	2.57	2.51
19	LW	3.4	2.94	2.87	**43**	FF	3.1	3.04	3.13
20	LY	2.46	2.37	2.4	**44**	FY	3.13	2.66	2.66
21	IG	1.68	1.22	1.25	**45**	WE	1.56	2.11	1.91
22	IA	1.68	1.8	1.65	**46**	WW	3.6	3.42	3.26
23	IV	2.05	2.06	2.19	**47**	YL	2.4	2.42	2.51
24	IL	2.26	2.39	2.5	**48**	SL	1.49	1.71	1.65

The r^2 for activities predicted by ISA–ECI vs the z-values of 0.90 shows that the two variables give similar results, but the ISA–ECI model has more degrees of freedom than the model with z-values.

Bitter Tasting Dipeptides. A set of 48 dipeptides with reported bitter tasting thresholds was investigated. Each dipeptide was parameterized with the ISA and ECI which gave a descriptor matrix with 48 objects (dipeptides) and 4 variables. As with the other data sets, prior to PLS analysis, the descriptor data were autoscaled. The first latent variable explained 78.1% of the y-variance, while the second component explained 6.7%, that is, the biological activity data are largely explained by the first latent variable. The observed and calculated bitterness data are shown in Table 6 and Figure 10 for both the ISA and ECI descriptors and the z-scales (RSD = 0.24 and 0.26, respectively). ISA–ECI do as well as the z-scales (r^2 = 0.93), using only four variables instead of six.

The **X**-loadings (Table 7) denote that the most important factors in the model are ECI at position 1 and ISA at position 2, with a contribution from ISA for the first amino acid position. All loadings are positive which indicates that highly bitter dipeptides should have hydrophobic amino acids in both positions, such as Phe

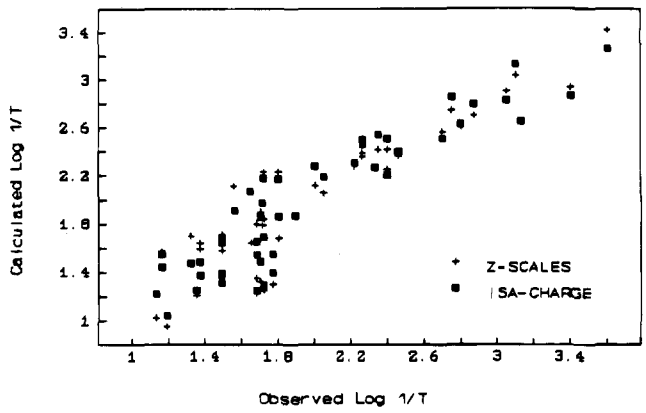

Figure 10. Plot of bitter thresholds for dipeptides described by ISA–ECI and z-scales.

Table 7. PLS Loadings for Bitter Tasting Dipeptides

	PLS components	
variable	1	2
ISA-1	0.51	−0.06
ECI-1	0.60	−0.86
ISA-2	0.67	0.47
ECI-2	0.17	−0.45

or Trp, as well as polar amino acids in position 1, as, for example, Asp or Arg. The highly bitter dipeptides in the data set have large ISA values, which are most appropriate for increasing the bitterness of dipeptides. Examples are compounds **44** and **46** where the amino acids Phe, Trp, Lys, and Tyr lead to highly bitter compounds. In an investigation on this set of 48 dipeptides,[12,14] each dipeptide was parameterized with the z-scales, the former using z-scales that have been extended to cover 35 unnatural amino acids and the latter using the z-values extracted from the 20 natural amino acids. With the extended z-scales, Jonsson et al.[14] report a one-dimensional PLS model that explained approximately 78% of the variation in the intensity of bitterness. A good agreement with observed bitterness was reported. Modeling of the 48 dipeptides by Hellberg et al.[12] resulted in a two-component PLS model which corroborated with earlier studies that the most important factors were hydrophobicity and size for both amino acid positions.

Angiotensin-Converting Enzyme (ACE) Inhibitors. A set of 58 dipeptides inhibiting ACE was obtained from the report of Hellberg et al.[12] The dipeptides and the ACE inhibition data in their study were taken from a compilation by Cushman et al.[33] and synthesized as part of the development of Captopril. Each of these dipeptides inhibiting ACE was parameterized with ISA and ECI, according to the amino acid sequence. The first and second PLS components explain 65% and 4% of the y-variance, respectively. The model was employed to calculate the inhibitory activity of the dipeptides, given in Table 8. The observed activity for ACE-inhibiting dipeptides is plotted against the calculated activity in Figure 11. There is good agreement ($r^2 = 0.70$), except for compounds **19**, **55**, and **56**. This deviation has also been previously observed[12] and may be due to assaying the cyclized form of the dipeptide. It has been noted that cyclization commonly occurs for dipeptides containing lipophilic amino acids such as Ile and Phe. Figure 12 is a plot of the calculated activities using the z-scales and the ISA–ECI descriptors, which

Table 8. Biological Activity for Angiotensin-Converting Enzyme Inhibitors

			calcd log 1/IC_{50}					calcd log 1/IC_{50}	
no.	peptide	obsd by 1/IC_{50}	$z_1z_2z_3$	ISA–ECI	no.	peptide	obsd by 1/IC_{50}	$z_1z_2z_3$	ISA–ECI
1	VW	5.8	4.78	4.74	**30**	KG	2.49	2.12	2.34
2	IW	5.7	4.99	4.93	**31**	FG	2.43	2.72	2.84
3	IY	5.43	4.29	4.21	**32**	GS	2.42	2.25	2.03
4	AW	5	4.42	4.37	**33**	GV	2.34	2.68	2.91
5	RW	4.8	4.56	4.5	**34**	MG	2.32	2.44	2.5
6	VY	4.66	4.08	4.02	**35**	GK	2.27	2.46	2.94
7	GW	4.52	4	4.09	**36**	GE	2.27	2.39	2.54
8	VF	4.28	4.42	4.36	**37**	GT	2.24	2.25	2.52
9	AY	4.06	3.73	3.65	**38**	WG	2.23	2.79	2.89
10	IP	3.89	4.14	3.81	**39**	HG	2.2	1.9	2.24
11	RP	3.74	3.7	3.38	**40**	GQ	2.15	2.49	2.45
12	AF	3.72	4.07	3.99	**41**	GG	2.14	1.63	1.75
13	GY	3.68	3.3	3.37	**42**	QG	2.13	2.02	1.91
14	AP	3.64	3.57	3.25	**43**	SG	2.07	1.82	1.81
15	RF	3.64	4.2	4.13	**44**	LG	2.06	2.62	2.62
16	VP	3.38	3.92	3.62	**45**	GD	2.04	2.52	2.38
17	GP	3.35	3.14	2.97	**46**	TG	2	2.04	2.08
18	GF	3.2	3.64	3.71	**47**	EG	2	1.84	1.97
19	IF	3.03	4.64	4.55	**48**	DG	1.85	1.66	1.89
20	VG	2.96	2.41	2.4	**49**	PG	1.77	2.18	2.42
21	IG	2.92	2.62	2.59	**50**	LA	3.51	3.47	3.11
22	GI	2.92	3.06	3.24	**51**	KA	3.42	2.97	2.84
23	GM	2.85	3.03	3.18	**52**	RA	3.34	3.04	2.66
24	GA	2.7	2.48	2.25	**53**	YA	3.34	3.27	3.05
25	YG	2.7	2.42	2.55	**54**	AA	3.21	2.9	2.52
26	GL	2.6	3.12	3.3	**55**	FR	3.04	3.71	4.09
27	AG	2.6	2.06	2.03	**56**	HL	2.49	3.4	3.79
28	GH	2.51	2.74	2.79	**57**	DA	2.42	2.51	2.39
29	GR	2.49	2.61	2.99	**58**	EA	2	2.69	2.47

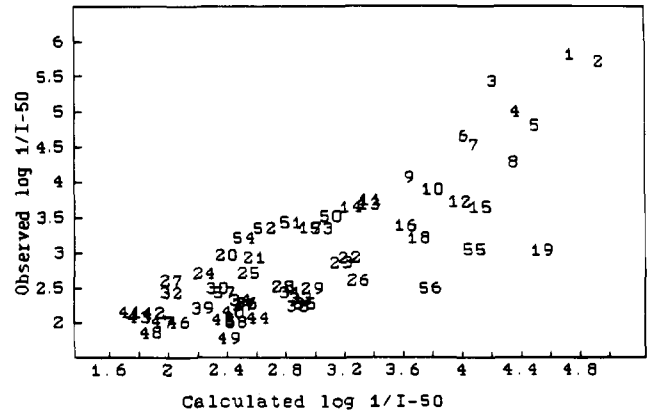

Figure 11. Biological activity of ACE inhibitors using ISA–ECI.

shows that ISA–ECI is comparable to the z-scales for parameterizing the structural variability ($r^2 = 0.94$).

From the plot of the first latent variables, t_1 vs u_1 given in Figure 13, it can be seen that dipeptides **1–8** are separated from the rest of the compounds. This cluster of dipeptides has Trp, Tyr, and Phe in position 2. The **X**-loadings indicate that the major source of variation is ISA in position 2 with some contribution from ECI. Hence, a highly active peptide should have an amino acid with a large, hydrophobic, aromatic amino acid with a polar functional group in position 2.

Using z_1, z_2, and z_3 as descriptors, a two-component PLS model was obtained by Hellberg and co-workers.[12] According to the absolute magnitude of the loadings, the most important factors were z_1 and z_2 at position 2 followed by z_3 and z_1 for position 1.

An earlier structure–activity relationship study[34] of ACE inhibitors indicated that Pro and aromatic side chains of Tyr and Phe are favored in position 2 or at

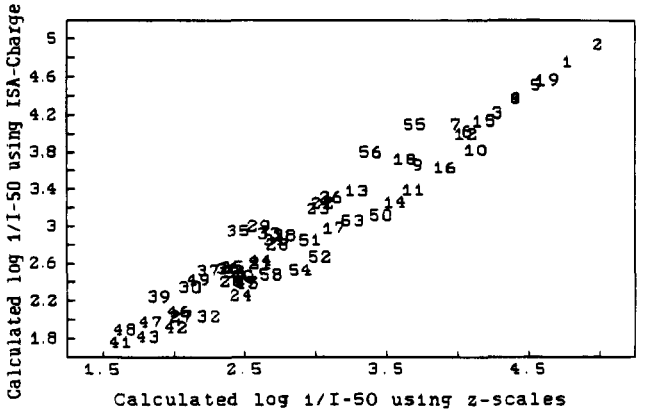

Figure 12. Plot of activity of ACE inhibitors using ISA–ECI and z-scales.

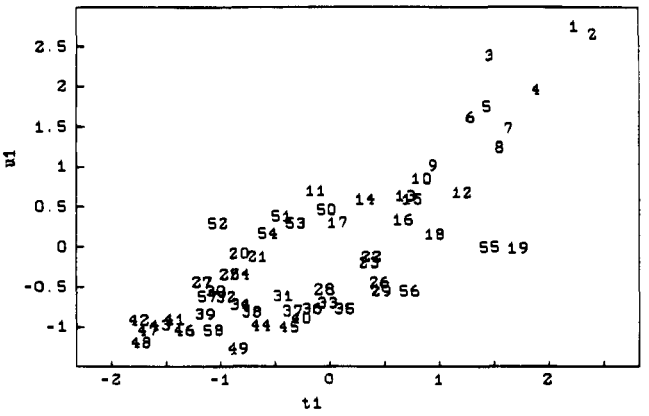

Figure 13. Plot of first latent variables t_1 and u_1 from **X** and **Y** blocks, respectively.

the C-terminal end of dipeptides while branched-chain aliphatic amino acids like Ile and Val are most effective at the N-terminal. It was concluded that both positions 1 and 2 have hydrophobic interactions with the ACE, which is consistent with our results.

Peptides with Unnatural Amino Acids. Oxytocin Antagonists. Potent, reversible antagonists of oxytocin are clinically useful as inhibitors of preterm labor. Flouret and co-workers[35] have designed the oxytocin parent antagonist (PA), Pmp^1-D-Trp^2-Ile^3-Glu^4-Asn^5-Cys^6-Pro^7-Arg^8-Gly^9-NH_2, where Pmp is pentamethylenemercaptopropionic acid. This compound displays strong potency on the rat uterus, displays low antidiuretic activity, and inhibits spontaneous uterine contractions in pregnant baboons. To enhance antagonism and/or decrease breakdown by tissue peptidases, analogues of this parent antagonist substituted with D-amino acids at positions 3–8 were synthesized.[36] These analogues were tested as antagonists of oxytocin in a uterotonic assay in the presence of magnesium salts. An examination of structure-activity relationships shows that analogues with substitutions at positions 3–5 in the ring portion were weaker antagonists than the parent molecule or were inactive. The analogue with Cys^6 replaced with D-Cys^6 is 3 times as potent as the parent antagonist. Replacement with D-amino acids in the tail portion (positions 6–8) gave analogues which were equipotent as the parent antagonist.

In this set of peptides, there were six varied positions which were described with ISA–ECI. The activity data from the rat oxytocic assay are expressed as pA_2. Table 9 lists the ISA and ECI descriptors derived from the D-amino acids and the rat oxytocic assay of the analogues.[36]

Table 9. Oxytocin Antagonists

				pA_2	
no.	analogue	ISA	charge	obsd	calcd
1	PA			7.77	7.88
2	D-Ile^3	154.69	0.11	5.23	5.24
3	D-aIle^3	149.31	0.12	5.11	5.14
4	D-Gln^4	25.57	1.35	5.24	5.30
5	D-Thr^4	45.62	0.66	4.95	4.95
6	D-Asn^4	24.08	1.31	5.41	5.28
7	D-Glu^4	39.81	1.3	0	4.4
8	D-Cit^4	47.24	1.9	5.51	5.53
9	D-Asn^5	24.08	1.31	0	−0.041
10	D-Cys^6	95.62	0.09	8.29	8.29
11	D-Pen^6	169.12	0.09	7.98	7.92
12	D-Pro^7	122.92	0.16	7.85	7.86
13	D-Arg^8	50.1	1.76	7.91	7.84

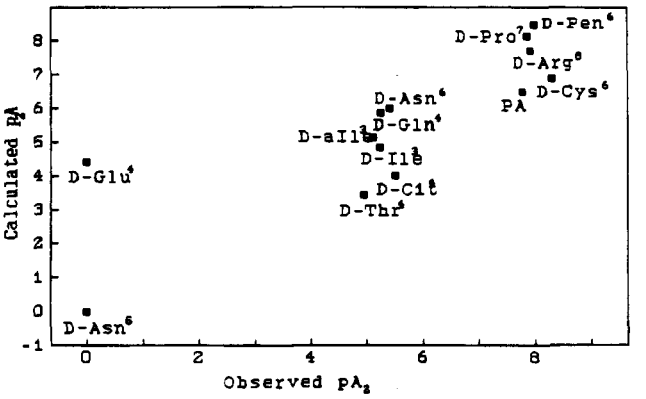

Figure 14. Plot of observed and calculated pA_2 of oxytocin antagonists.

The PLS analysis resulted in a two-dimensional model describing 68% of the variance in oxytocic activity. The plot between observed and calculated pA_2 values is given in Figure 14 and clearly shows two clusters of peptides—the comparatively weak oxytocic antagonists substituted at positions 3 and 4 and the more potent analogues substituted at positions 6–8. Such distributions can yield good correlation statistics, but the models are between the means of the two clusters. A QSAR analysis for each of the two groups was thus performed.

The PLS analysis of the group substituted at positions 3 and 4 resulted in a two-dimensional model describing 89% (79% and 10%, respectively) of the variance in biological activity. There is very good agreement between observed and calculated antagonistic potency (Table 9). The descriptor which mainly contributes to the PLS model is the ECI at position 4 with a small contribution from ISA at both positions 3 and 4. In another study of anti-oxytocin activities using the intermolecular force parameters,[6] it was found that ionic side chains and hydrogen bonding dominate the structural effects, with small but significant steric contributions from branching of the side chain.

The PLS analysis of the group substituted at positions 6–8 gave a three-component model explaining 87% of the variance in antagonist potency with the contribution from each 39%, 28%, and 20%, respectively. The calculated activities are given in Table 9. The highest contribution to the model, according to the absolute magnitude of the PLS loadings, is given by ISA–ECI in position 6 with contributions from ISA–ECI in position 8. Flouret et al.[36] have likewise shown that

high antagonist potency resulted from the replacement of Cys[6] with D-Pen[6] and D-Cys[6]. The result appears to indicate that Cys[6] is not one of the essential components of the oxytocin ring for recognition by the oxytocin receptor. Further, with a D-amino acid, the configuration changes the direction of the tail peptide with respect to the tail of the tocin 20-membered ring. Hence, D-Cys[6] shows different binding requirements than the L-form. It should be noted that only a small number of variants is available for each group, six for the first and five for the second. However, the advantage of a QSAR study is that it provides an indication of all possible, relevant amino acid changes that may be responsible for the variation in biological activity. This suggests position 6 to be of importance.

Tachykinins. The tachykinins are a family of peptides with a common C-terminal sequence, Phe-X-Gly-Leu-Met-NH_2. Three tachykinins have been established as having a transmitter role in mammalian tissues: substance P (SP), neurokinin A (NKA), and neurokinin B (NKB). Substance P induces hypotension and salivation and is involved in pain transmission; neurokinin A is a potent spasmogenic agent at both the bronchial and gastrointestinal level, while neurokinin B modulates the release of neurotransmitters. Three distinct receptors, NK-1, NK-2, and NK-3, mediate the biological effects of the tachykinins in mammalian tissues where SP, NKA, and NKB are the most potent natural ligands, respectively.

Since NK-2 receptors are involved in the spasmogenic effect of tachykinins on human smooth muscles, there has been considerable interest in the development of selective NK-2 antagonists. Clementi et al.[26] used the C-terminal heptapeptide of NKA, that is, NKA-(4−10), as a template to develop antagonists with good selectivity for NK-2. D-Trp was introduced in positions 6 and 8 of NKA-(4−10) to develop potent antagonists with good selectivity for NK-2 receptors as compared to NK-1 and NK-3 receptors. The biological activity of these peptides was determined in three preparations: the isolated rat vas deferens (RVD), the rabbit pulmonary artery (RPA), and the hamster isolated trachea (HT) which contains only NK-2 receptors and was investigated to study the effect of tachykinin-related peptides on a smooth muscle airway. Table 10 lists the pA_2 values for the antagonist activity of the 24 heptapeptides in the three bioassays for NK-2 receptors.[26]

Separate QSAR models were obtained for each reported activity in order to investigate whether there is any difference in the bioassay behavior which could be related to the structural features of this peptide set. Three-component PLS models were obtained which explain 87%, 45%, and 60% of the antagonistic activity using the RVD, RPA, and HT bioassays, respectively. The models were employed to calculate the biological activities in the three preparations, which are given in Table 10. Good agreement between the values was obtained for the RVD ($r^2 = 0.87$). In all three models, the highest contribution, according to the absolute magnitude of the PLS loadings, was given by ISA−ECI relative to positions 7−9 of NKA-(4−10), as well as ECI at position 6. The loadings for the first component are illustrated in Figure 15 for the three bioassays. On the basis of this set of analogues, it is not possible to pinpoint any single amino acid position that could account for any difference in the bioassay behavior.

Table 10. List of Antagonist Activity in Three Bioassays

		antagonist activity					
		obsd			calcd		
no.	tachykinin analogue	RVD	RPA	HT	RVD	RPA	HT
1	DwFwGLM	5.11	5.23	5.04	5.02	4.4	4.86
2	DYFwGLM	4.85	4	4.83	5.1	4.92	5.06
3	DYwVwwR	6.6	7.65	5.8	6.03	6.1	5.60
4	DYWVwwR	4.59	4	4.81	4.92	4.25	4.85
5	DYPVwwR	5.36	4.89	4.76	5.47	4.94	4.55
6	Dywvwwr	6.07	6.39	5.96	6.39	6.53	5.74
7	DYwVGwR	4.73	4.71	5.2	4.66	4.5	5.13
8	Dywvgwr	6.42	6.58	6.25	6.1	6.02	5.58
9	DYwVwLR	6.65	6.72	6.19	6.28	6.28	5.56
10	NYwVwwR	6.46	7.19	5.93	6.52	7.25	5.94
11	DYYVYYR	5.03	4	4	4.92	3.82	4.10
12	DYwVwwF	6.54	5.9	6.03	6.67	5.67	5.79
13	DYwVwww	6.81	5.79	5.86	6.67	5.49	5.76
14	DYwVwwY	6.72	4	5.76	6.41	5.87	5.72
15	DYwVwwM	6.42	7.05	5.84	6.45	5.99	5.74
16	DSwVwwM	5.71	5.32	5.19	5.64	5.59	5.74
17	DWwVwwR	6.47	5.2	4.95	6.94	7.02	5.81
18	DwwVwwR	5.62	4	4.5	5.95	5.58	5.40
19	QYwVwwF		5.78	5.76	5.28	5.55	
20	DYwVwwE	7.51	5.58	6.37	5.62		
21	DYwVwwL	7.1	5.79	5.92	5.77		
22	DYwVwwG	7.46	5.83	6.85	5.71		
23	DYwAwwK	6.53	5.87	6.45	5.86		
24	DKwVwwK		4	5.38	5.64	5.61	

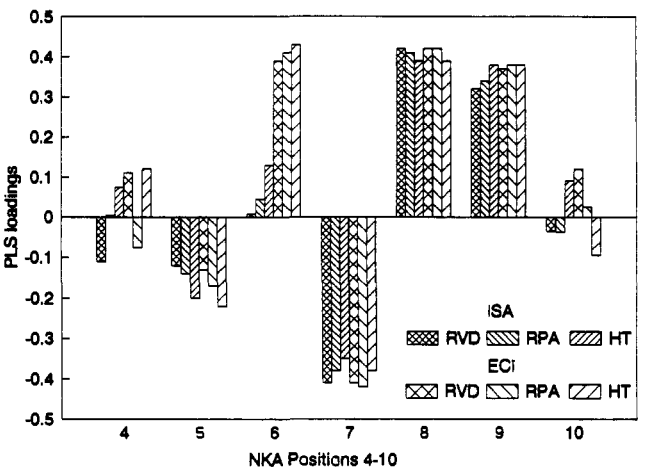

Figure 15. PLS loadings for the three bioassays for NK-2 receptors.

Conclusions

In this study a new set of amino acid side chain descriptors relevant to peptide QSAR studies is presented. These descriptors, ISA and ECI, are calculated from the three-dimensional structure of the amino acids and their analogues. Their derivation is straightforward, and it is easy to interpret the QSARs which include them. ISA approximates the hydrophobic character of the side chain substituent, and ECI is a measure of the charge concentration of the amino acid. Such calculated variables strongly depend on conformation, but if they are computed in a consistent manner, they can be useful in QSAR studies. For the amino acids and analogues, the computation is relatively nonintensive. It also represents an integrated approach whereby the molecules are energy minimized by molecular mechanics and then subjected to semiempirical molecular orbital calculations. Finally, the resulting spatial coordinates are used as input to the computation of solvent accessible surface areas.

Correlations derived using ISA and ECI are comparable to those derived using the principal properties, and

they can easily be extended to synthetic unnatural amino acids or peptide mimetics which result from side chain modification of template peptides. They offer the advantage of requiring fewer descriptors and thus, compared to the *z*-values, result in more degrees of freedom. It has been shown that the composition of the training sets and test sets can have a substantial effect on the resulting correlations.[37] Future approaches will include applying the techniques of statistical design in the selection of peptide analogues, hence increasing the utility of this QSAR as a pharmacological prescreen for biological activity.

Acknowledgment. We thank Dr. A. J. Hopfinger for helpful discussions and for the use of the CHEM-LAB-II molecular modeling software.

References

(1) Sneath, P. H. A. Relations Between Chemical Structure and Biological Activity in Peptides. *J. Theor. Biol.* **1966**, *12*, 157–195.
(2) Nadasdi, L.; Medzihradszky, K. A Study of the Applicability of QSAR Calculation for Peptide Hormones. *Biochem. Biophys. Res. Commun.* **1981**, *99*, 451–457.
(3) Borea, P. A.; Santo, G. P.; Salvadori, S.; Tomatis, R. Opioid Peptides. Pharmacological Activity and Lipophilic Character of Dermorphin Oligopeptides. *Farmaco, Ed. Sci.* **1983**, *38*, 521–526.
(4) Asao, M.; Iwamura, H.; Akamatsu, M.; Fujita, T. Quantitative Structure-Activity Relationships of the Bitter Thresholds of Amino Acids, Peptides, and their Derivatives. *J. Med. Chem.* **1987**, *30*, 1873–1879.
(5) Fauchere, J.; Charton, M.; Kier, L. B.; Verloop, A.; Pliska, V. Amino Acid Side Chain Parameters for Correlation Studies in Biology and Pharmacology. *Int. J. Pept. Protein Res.* **1988**, *32*, 269–278.
(6) Charton, M. The Quantitative Description of Amino Acid, Peptide, and Protein Properties and Bioactivities. *Prog. Phys. Org. Chem.* **1990**, *18*, 163–284.
(7) DePriest, S. A.; Mayer, D.; Naylor, C. D.; Marshall, G. R. 3D-QSAR of Angiotensin-Converting Enzyme and Thermolysin Inhibitors: A Comparison of CoMFA Models Based on Deduced and Experimentally Determined Active Site Geometries. *J. Am. Chem. Soc.* **1993**, *115*, 5372–5384. Waller, C. L.; Oprea, T. I.; Giolitti, A.; Marshall, G. R. Three-Dimensional QSAR of Human Immunodeficiency Virus (I) Protease Inhibitors. 1. A CoMFA Study Employing Experimentally-Determined Alignment Rules. *J. Med. Chem.* **1993**, *36*, 4152–4160. Waller, C. R.; Marshall, G. R. Three Demensional Quantititative Structure Activity Relationship of Angiotensin-Converting Enzyme and Thermolysin Inhibitors. II A Comparision of CoMFA Models Incorporating Molecular Orbi8al Fields and Desolvation Free Energies Based on Active-Analog and Complemenatary-Receptor-Field Alignment. *J. Med. Chem.* **1993**, *36*, 2390–2403.
(8) Charton, M.; Charton, B. I. The Dependence of the Chou-Fasman Parameters on Amino Acid Side Chain Structure. *J. Theor. Biol.* **1983**, *102*, 121–134.
(9) Kidera, A.; Konishi, Y.; Oka, M.; Ooi, T.; Scheraga, H. A. Statistical Analysis of the Physical Properties of the 20 Naturally Occurring Amino Acids. *J. Protein Chem.* **1985**, *4*, 23–55.
(10) Hellberg, S.; Sjöström, M.; Skagerberg, B.; Wold, S. Peptide Quantitative Structure-Activity Relationships, a Multivariate Approach. *J. Med. Chem.* **1987**, *30*, 1126–1135.
(11) Hellberg, S.; Sjöström, M.; Wold, S. The Prediction of Bradykinin Potentiating Potency of Pentapeptides. An Example of a Peptide Quantitative Structure-Activity Relationship. *Acta Chem. Scand. B* **1986**, *40*, 135–140.
(12) Hellberg, S.; Eriksson, L.; Jonsson, J.; Lindgren, F.; Sjöström, M.; Skakerberg, B.; Wold, S.; Andrews, P. Minimum Analogue Peptide Sets (MAPS) for Quantitative Structure-Activity Relationships. *Int. J. Pept. Protein Res.* **1991**, *37*, 414–424.
(13) Wold, S.; Eriksson, L.; Hellberg, S.; Jonsson, J.; Sjöström, M.; Skagerberg, B.; Wikström, C. Principal Property Values for Six Non-natural Amino Acids and their Application to a Structure-Activity Relationship for Oxytocin Peptide Analogues. *Can. J. Chem.* **1987**, *65*, 1814–1820.
(14) Jonsson, J.; Eriksson, L.; Hellberg, S.; Sjöström, M.; Wold, S. Multivariate Parametrization of 55 Coded and Non-coded Amino Acids. *Quant. Struct.-Act. Relat.* **1989**, *8*, 204–209.
(15) Grigoras, S. A New Semiempirical Method for the Calculation of the Partition Coefficient. Ph.D. Thesis, University of Illinois at Chicago, Chicago, IL, 1985.
(16) Suzuki, S.; Green, P. G.; Bumgarner, R. E.; Dasgupta, S.; Goddard, W. A., III; Blake, G. A. Benzene forms Hydrogen Bonds with Water. *Science* **1992**, *257*, 942–945.
(17) Dunn, W. J., III; Koehler, M. G.; Grigoras, S. The Role of Solvent-Accessible Surface Area in Determining Partition Coefficients. *J. Med. Chem.* **1987**, *30*, 1121–1126.
(18) Buydens, L.; Massart, D. L.; Geerlings, P. Prediction of Gas Chromatographic Retention Indexes with Topological, Physicochemical, and Quantum Chemical Parameters. *Anal. Chem.* **1983**, *55*, 738–744.
(19) Buydens, L.; Massart, D. L.; Geerlings, P. Relationship between Gas Chromatographic Behavior and Topological, Physicochemical, and Quantum Chemically Calculated Charge Parameters for Neuroleptica. *J. Chromatogr. Sci.* **1985**, *23*, 304–307.
(20) Pearlstein, R. A. *CHEMLAB-II Users Guide, v. 11.0*, 1988, Chemlab Inc., 1780 Wilson Dr., Lake Forest, IL 60045.
(21) Weiner, S. J.; Kollman, P. A.; Case, D. A.; Singh, C. U.; Ghio, C.; Alagona, G.; Profeta, S. J.; Weiner, P. A New Force Field for Molecular Mechanical Simulation of Nucleic Acid and Proteins. *J. Am. Chem. Soc.* **1984**, *106*, 765–784.
(22) Pople, J. A.; Beveridge, D. C. *Approximate Molecular Orbital Theory*; McGraw Hill: New York, 1970.
(23) Koehler, M. G.; Grigoras, S.; Dunn, W. J. The Relationship between Chemical Structure and the Logarithm of the Partition Coefficient. *Quant. Struct.-Act. Relat.* **1988**, *7*, 150–159.
(24) Pearlman, R. *Program No. 432*, SAREA Bloomington, IN, Quantum Chemistry Program Exchange, 1981.
(25) Wold, S.; Dunn, W. J., III. Multivariate QSARs: Conditions for their Applicability. *J. Chem. Inf. Comput. Sci.* **1983**, *23*, 6–13.
(26) Clementi, S.; Cruciani, G.; Riganelli, D.; Rovero, P.; Pestellini, V.; Maggi, C. A.; Baroni, M. Chemometric Approach to a QSAR Study of Peptides Behaving as NK-2 Receptor Antagonists. *Tetrahedron Comput. Methodol.* **1990**, *3*, 379–387.
(27) Glen, W. G.; Sarker, M.; Dunn, W. J., III; Scott, D. R. UNIPALS: Software for Principal Components Analysis and Partial Least Squares Regression. *Tetrahedron Comput. Methodol.* **1989**, *2*, 377–396.
(28) Wolfenden, R.; Andersson, L.; Cullis, P. M.; Southgate, C. C. B. Affinities of Amino Acid Side Chains for Solvent Water. *Biochemistry* **1981**, *20*, 849–855.
(29) Fauchere, J.; Pliska, V. Hydrophobic Parameters of Amino Acid Side Chains from the Partitioning of N-Acetyl-Amino-Acid Amides. *Eur. J. Med. Chem.* **1983**, *4*, 369–375.
(30) Radzicka, A.; Wolfenden, R. Comparing the Polarities of the Amino Acids: Side-chain Distribution Coefficients between the Vapor Phase, Cyclohexane, 1-Octanol, and Neutral Aqueous Solution. *Biochemistry* **1988**, *27*, 1664–1670.
(31) Ufkes, J. G. R.; Visser, B. J.; Heuver, G.; van der Meer, C. Structure-Activity Relationships of Bradykinin Potentiating Peptides. *Eur. J. Pharmacol.* **1978**, *50*, 119–122.
(32) Ufkes, J. G. R.; Visser, B. J.; Heuver, G.; Wynne, H. J.; van der Meer, C. Further Studies on the Structure-Activity Relationships of Bradykinin-Potentiating Peptides. *Eur. J. Pharmacol.* **1982**, *79*, 155–158.
(33) Cushman, D. W.; Ondetti, M. A.; Cheung, H. S.; Antonaccio, M. J.; Murthy, V. S.; Rubin, B. Inhibitors of Angiotensin-Converting Enzyme. *Adv. Exp. Med. Biol.* **1980**, *130*, 199–225.
(34) Cheung, H. S.; Wang, F. L.; Ondetti, M. A.; Sabo, E. F.; Cushman, D. W. Binding of Peptide Substrates and Inhibitors of Angiotensin-Converting Enzyme. *J. Biol. Chem.* **1980**, *255*, 401–407.
(35) Flouret, G.; Brieher, W.; Mahan, K.; Wilson, L. Design of Potent Oxytocin Antagonists Featuring D-Tryptophan at Position 2. *J. Med. Chem.* **1991**, *34*, 642–646.
(36) Flouret, G.; Majewski, T.; Brieher, W.; Wilson, L. Systematic Substitution of an Oxytocin Antagonist with D-Amino Acids: Unexpected High Antagonistic Potency of the D-Cys^6-Substituted Analogue. *J. Med. Chem.* **1993**, *36*, 747–749.
(37) Wold, S.; Sjöström, M.; Carlson, R.; Ludstedt, T.; Hellberg, S.; Skagerberg, B.; Wikström, C.; Öhman, J. Multivariate Design. *Anal. Chim. Acta* **1986**, *191*, 17–32.

JM940468A